Current Biology 24, 1978–1984, September 8, 2014 ©2014 Elsevier Ltd All rights reserved http://dx.doi.org/10.1016/j.cub.2014.07.020

Report

Presynaptic Gain Control Drives Sweet and Bitter Taste Integration in *Drosophila*

Bonnie Chu,[1] Vincent Chui,[1] Kevin Mann,[1] and Michael D. Gordon[1,*]

[1]Department of Zoology, Cell and Developmental Biology, University of British Columbia, Vancouver, BC V6T 1Z3, Canada

Summary

The sense of taste is critical in determining the nutritional suitability of foods. Sweet and bitter are primary taste modalities in mammals, and their behavioral relevance is similar in flies. Sweet taste drives the appetitive response to energy sources, whereas bitter taste drives avoidance of potential toxins and also suppresses the sweet response [1, 2]. Despite their importance to survival, little is known about the neural circuit mechanisms underlying integration of sweet and bitter taste. Here, we describe a presynaptic gain control mechanism in *Drosophila* that differentially affects sweet and bitter taste channels and mediates integration of these opposing stimuli. Gain control is known to play an important role in fly olfaction, where $GABA_B$ receptor ($GABA_BR$) mediates intra- and interglomerular presynaptic inhibition of sensory neuron output [3–5]. In the taste system, we find that gustatory receptor neurons (GRNs) responding to sweet compounds express $GABA_BR$, whereas those that respond to bitter do not. $GABA_BR$ mediates presynaptic inhibition of calcium responses in sweet GRNs, and both sweet and bitter stimuli evoke GABAergic neuron activity in the vicinity of GRN axon terminals. Pharmacological blockade and genetic reduction of $GABA_BR$ both lead to increased sugar responses and decreased suppression of the sweet response by bitter compounds. We propose a model in which GABA acts via $GABA_BR$ to expand the dynamic range of sweet GRNs through presynaptic gain control and suppress the output of sweet GRNs in the presence of opposing bitter stimuli.

Results and Discussion

To investigate the role of presynaptic inhibition in fly taste we began by examining the expression of $GABA_B$ receptor ($GABA_BR$), an obligate heterodimer in *Drosophila* composed of $GABA_BR1$ and $GABA_BR2$ [6]. Using the *$GABA_BR2$-Gal4* reporter [5], we observed expression in 49 ± 1 gustatory receptor neurons (GRNs) per labial palp of the proboscis (Figure 1A; n = 26 palps). Colabeling with specific reporters for sweet (*Gr64f-LexA*), bitter (*Gr66a-LexA*), and water (*ppk28-LexA*) neurons revealed expression of *$GABA_BR2$-Gal4* in most sweet (88%) and very few bitter (6%) or water (2%) GRNs (Figures 1B–1E). Although we do not have a Gal4-independent reporter for the *ppk23*-expressing pheromone-responsive neuron population [7, 8], flies carrying both *$GABA_BR2$-Gal4* and *ppk23-Gal4* showed expression in 49 ± 3 GRNs (Figure S1 available online; n = 6 labial palps), demonstrating that most, if not all, *ppk23-Gal4* neurons also express *$GABA_BR2$-Gal4*. Moreover, *ppk23-Gal4* is expressed in 22 ± 2 GRNs per labial palp [7], which corresponds precisely with the number of *$GABA_BR2$*-expressing GRNs not labeled by *Gr64f-LexA* (Figure 1E). This suggests that sweet and pheromone-responsive GRNs account for almost all of the *$GABA_BR2$*-expressing population. The small number of *Gr66a-LexA*- and *ppk28-LexA*-positive GRNs observed to express *$GABA_BR2$-Gal4* most likely reflects very slight unfaithfulness of the reporters in recapitulating endogenous receptor expression, as this was not consistently observed in different individuals.

Because sweet and bitter neurons drive opposing behavioral responses and express substantially different levels of presynaptic $GABA_BR2$, we decided to focus on the potential role of presynaptic inhibition in these two sensory neuron populations. GRN axons terminate in the subesophageal zone (SEZ) of the fly brain, where they are thought to synapse with yet-unidentified second-order gustatory projection neurons and most likely also connect to local interneurons [9–11]. We observed expression of the GABAergic-specific driver *GAD1-Gal4* in several hundred neurons in the region of the SEZ, with most being located dorsally and laterally (Figure 2A). GFP reconstitution across synaptic partners (GRASP [9, 12]) revealed that both sweet and bitter GRNs make extensive contact with GABAergic neuronal processes in the SEZ neuropil, suggesting the existence of functional connections between GRNs and local inhibitory interneurons (Figures 2B and 2C). To examine whether GABAergic interneurons in close proximity to GRN axon terminals show taste-evoked activity, we expressed the genetically encoded calcium sensor GCaMP3 under the control of *GAD1-Gal4*. Changes in fluorescence were then measured using confocal imaging of an in vivo fly preparation exposed to labellar stimulation with water, sucrose, and the bitter compound L-canavanine (Figures 2D–2G). Sparse responses were regularly observed to taste stimulations, with zero to four neurons showing taste-evoked activity in each selected optical section. Twenty-four of 36 observed taste-responsive GABAergic neurons were excited by both sweet and bitter stimuli, whereas nine responded to either sweet (seven) or bitter (two), but not both (Figure 2F). Additionally, 22 of the 36 neurons measured showed at least a small response to water, which is both the solvent for the tested taste compounds and a distinct taste modality detected by a dedicated population of gustatory neurons [13–15]. This includes 15 cells that responded to all three stimuli, some of which may have been excited by nongustatory cues present during stimulation. Mapping of GABAergic neuron position in the SEZ showed no obvious connection between position and receptive field, indicating that taste responses are broadly distributed in this population (Figures 2G and S2A). However, somatic calcium changes observed in *GAD1*-expressing neurons were always accompanied by broader responses in the neuropil of the SEZ, often in areas closely associated with GRN axon terminals (Figures 2E, S2B, and S2C). Quantification of neuropil calcium changes in the region of GRN axon terminals revealed similar responses to both sweet and bitter stimuli (Figure 2H). Together, these data suggest that individual

*Correspondence: gordon@zoology.ubc.ca

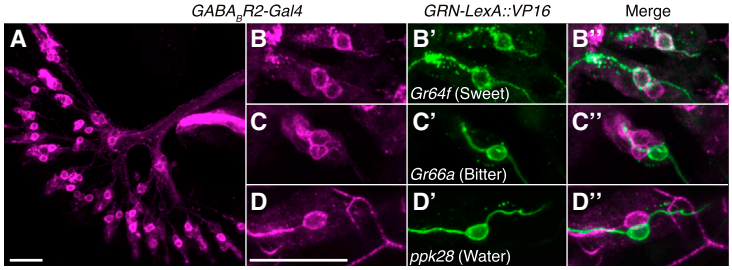

E

GRN type	GRN marker$^+$ GABA$_B$R2$^+$	GRN marker$^+$ GABA$_B$R2$^-$	GRN marker$^-$ GABA$_B$R2$^+$	Proportion of GRN type that expresses GABA$_B$R2
Sweet	26 +/- 1	4 +/- 1	22 +/- 2	88 +/- 2%
Bitter	1 +/- 1	19 +/- 1	48 +/- 2	6 +/- 1%
Water	0.3 +/- 0.2	15 +/- 1	46 +/- 3	2 +/- 0.5%

Figure 1. A Subset of GRN Classes Expresses GABA$_B$R2

(A–D) Single labial palp (A) or representative individual sensilla (B–D) from flies expressing CD8::tdTomato (magenta) under the control of *GABA$_B$R2-Gal4* and CD2::GFP (green) under the control of *Gr64f-LexA::VP16* (B′, sweet), *Gr66a-LexA::VP16* (C′, bitter), or *ppk28-LexA::VP16* (D′, water). Merged images re shown in (B″), (C″), and (D″). Scale bars, 20 μm.

(E) The number of GRNs per labial palp coexpressing *GABA$_B$R2-Gal4* and each GRN marker, the number expressing each GRN marker alone, the number expressing *GABA$_B$R2-Gal4* without the labeled GRN marker, and the proportion of each GRN class observed to express *GABA$_B$R2-Gal4*. Values represent mean ± SEM; n = 6 palps per genotype.

See also Figure S1.

SEZ GABAergic interneurons can be broadly or narrowly tuned to taste stimuli and that gustatory input may evoke GABA release in the vicinity of GRN axon terminals.

To examine the functional properties of GABA$_B$R expressed in GRNs, we measured calcium responses of GRN axon terminals in the SEZ using GCaMP3. Importantly, calcium changes at the axon terminals should reflect both stimulus-driven excitation of the GRNs and synaptic modulation present in the system [5, 16]. Gr64f (sweet) GRN terminals show robust calcium responses to stimulation of the proboscis with sucrose, and this response was blunted by the addition of the GABA$_B$R agonist SKF97541 (Figures 3A–3C). Application of the GABA$_B$R antagonist CGP54626 resulted in elevated responses to a series of sucrose concentrations (Figure 3D), suggesting that GABA$_B$R signaling mediates gain control of sweet GRN output in much the same way that it affects olfactory receptor neuron (ORN) output in the fly antennal lobe [3, 5, 17]. By contrast, addition of CGP54626 had no effect on the calcium response of *Gr66a*-expressing bitter neurons stimulated with denatonium (Figure 3E). These results demonstrate that sweet, but not bitter, GRNs receive GABA$_B$R-mediated presynaptic inhibition after stimulation with a cognate ligand.

To determine the behavioral consequences of GABA$_B$R's effects in sweet GRNs, we used the proboscis extension reflex (PER), an established assay of taste acceptance behavior [18]. Sweet GRN activation is sufficient to elicit PER and is necessary for the PER response to sugars [9, 10]. Moreover, PER is a quantitative readout of sweet GRN activation, with higher stimulus intensities eliciting greater GRN activity and a concomitant increase in extension probability [10, 16, 19–22]. Thus, modulation of sweet GRN output is expected to alter the PER response to sugars [16]. We knocked down *GABA$_B$R2* expression in sweet GRNs by driving *UAS-GABA$_B$R2(RNAi)* under the control of *Gr64f-Gal4* and measured PER over a series of sucrose concentrations. As predicted by our calcium imaging, flies with lowered GABA$_B$R2 levels in sweet GRNs showed elevated behavioral responses (Figure 3F). The same effect was observed over a series of glucose concentrations, supporting the role of GABA$_B$R in the processing of various nutritionally relevant sugars (Figure S3A). As an additional control, we used a second *UAS-RNAi* construct directed at a different region of *GABA$_B$R2* and saw the same effect (Figure S3B). By contrast, when we expressed *UAS-GABA$_B$R2 (RNAi)* in bitter neurons under the control of *Gr66a-Gal4,* we observed no change in sugar sensitivity (Figure 3G). For further confirmation of the relationship between increased GRN output and behavior, we plotted the sweet GRN calcium response versus PER for control flies and for flies subjected to GABA$_B$R knockdown or pharmacological inhibition (Figure S3C). This analysis supports the notion that the elevated sweet GRN output observed with calcium imaging after GABA$_B$R blockade underlies the elevated PER response observed after *GABA$_B$R2* knockdown in sweet GRNs.

Why would we observe a gain control mechanism in sweet, but not bitter, GRNs? One possibility is that intramodal GABA$_B$R-mediated inhibitory feedback acts to expand the dynamic range of sweet GRNs, defined here as the range of stimulus concentrations between the minimum detection threshold and saturation. This would enhance the fly's ability to accurately discriminate differences in sugar concentration over a wide range, providing a key selective advantage in the wild where energy sources may be limited and choosing the optimal food source is essential. Although our behavioral and calcium imaging data support this model, it is important to note that we lack the resolution required to precisely determine the saturation point for PER behavior with or without *GABA$_B$R2* knockdown; however, given the elevated responses at nonsaturating stimulus concentrations after *GABA$_B$R2* knockdown and the strong relationship between PER and sweet GRN output, we expect that GABA$_B$R function widens the stimulus range over which the fly shows a measurable change in behavior. Additionally, although PER behavior was close to saturated at a sucrose concentration of 100 mM in our assay, we would not expect behavioral saturation at this concentration in all contexts. The effective stimulus intensity range depends on a number of factors, including the specific behavior measured and the satiety state [16, 23]. Thus, changes in sweet GRN output at very high stimulus intensities are likely to be relevant in some situations. In contrast to sweet neurons, bitter neurons lacking presynaptic inhibition would be tuned to maximize sensitivity at the cost of dynamic range, thereby allowing the most robust and reliable avoidance of toxins that may be present at even very low concentrations. These effects are analogous to those observed in fly olfaction, where GABA$_B$R-mediated input gain control expands the dynamic range of many glomeruli in the antennal lobe but is lacking in the V glomerulus, which specifically responds to the aversive gas carbon dioxide [3–5, 24]. A second, not mutually

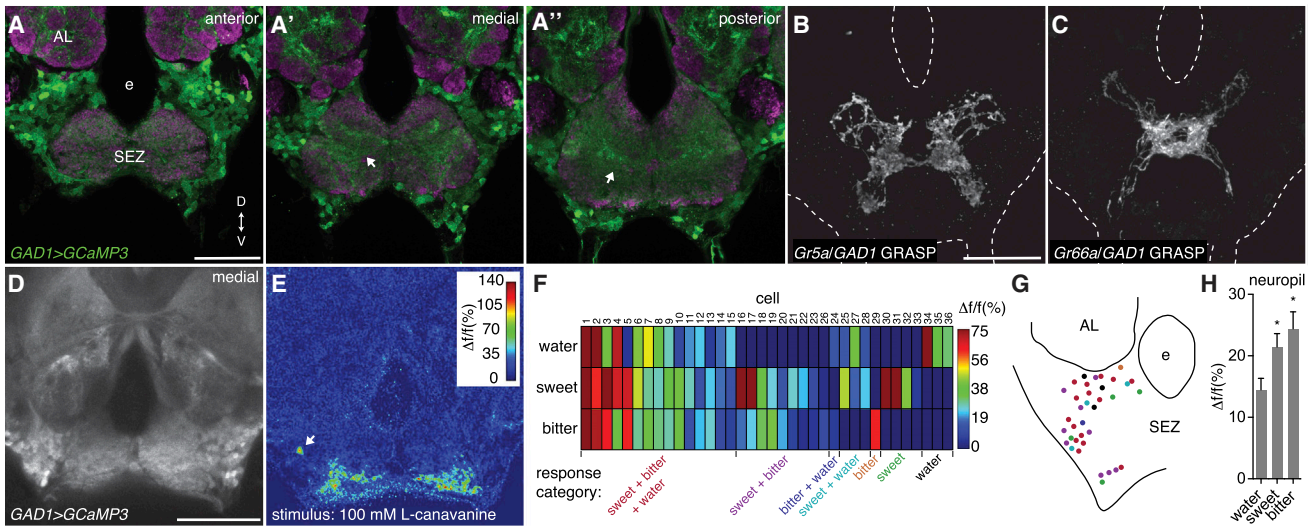

Figure 2. GRNs Are Functionally Connected to GABAergic Interneurons in the SEZ

(A) Immunofluorescence of GFP (green) and nc82 (neuropil, magenta) in the SEZ of a fly expressing GCAMP3 in GABAergic neurons under the control of *GAD1-Gal4*. Images are projections through 5 μm optical sections in the anterior half of the SEZ. Sections are spaced 5 μm apart and labels indicate relative position of each. Arrows indicate GABAergic processes in the region of GRN axons in (A′) and (A″).

(B and C) GRASP (grayscale) reveals contact between GABAergic interneurons and sweet (B) or bitter (C) GRN axon terminals. GABAergic interneurons express splitGFP1-10 under the control of *GAD1-Gal4*. GRNs express CD4::splitGFP11 under the control of *Gr5a-LexA::VP16* (B, sweet GRNs) or *Gr66a-LexA::VP16* (C, bitter GRNs). GRASP is detected using an antibody specific to the reconstituted form of GFP [9]. Dotted lines delineate the edges of brains.

(D) Baseline fluorescence in the SEZ of a fly expressing GCaMP3 in GABAergic interneurons.

(E) Heatmap showing change in GCaMP fluorescence following stimulation of the fly in (D) with the bitter compound L-canavanine at 100 mM. Arrow marks single cell body observed to respond. Note the widespread activation of neuronal processes within SEZ neuropil.

(F) Responses of 36 GABAergic neurons from 20 different flies to stimulation with water, sweet (100 mM sucrose) and bitter (100 mM L-canavanine). Cells are grouped by receptive field, with each category color-coded for mapping in (G).

(G) Cartoon of one side of the SEZ, with colored dots representing the position of each cell body with a response shown in (F). Dots are color-coded based on response categories shown in (F).

(H) Taste responses of GABAergic neuronal processes in the SEZ neuropil regions targeted by GRN axon terminals. Values represent mean ± SEM; n = 29 focal planes across 23 different flies. Asterisks indicate significant difference from water by one-way ANOVA with Bonferroni correction for multiple comparisons (*$p < 0.05$).

SEZ, subesophageal zone; AL, antennal lobe; e, esophagus. Scale bars, 50 μm. See also Figure S2 for the specific identity of each cell shown in the diagram of (G) and a second heatmap illustrating taste-evoked GABAergic responses in the SEZ neuropil.

exclusive possibility is that intermodal presynaptic inhibition of sweet GRNs is essential for integrating other sensory cues. For example, given that bitter tastes evoke activity in GABAergic SEZ neurons, the addition of bitter to a sweet solution could further inhibit sweet GRN output and therefore blunt the appetitive behavioral response. This would be critical to survival in the wild, where animals must react appropriately to palatable food sources laced with bitter, potentially harmful, substances.

In flies, many bitter compounds directly inhibit the activation of sweet GRNs [25, 26]. This effect requires the odorant-binding protein OBP49a, which binds to bitter compounds and is thought to interact with sugar receptors and inhibit their function [26]. However, artificial activation of bitter GRNs with a heterologous ligand/receptor pair in the absence of a bitter compound is sufficient to suppress flies' appetitive response to sugars, demonstrating that integration of sweet and bitter tastes must occur both at the receptor level and using downstream taste circuits [21, 27].

To investigate the possibility that presynaptic inhibition underlies suppression of sweet responses by bitter stimuli, we used L-canavanine, which, unlike the other bitter compounds tested, does not directly inhibit the firing rate of sweet GRNs [26]. By eliminating this cell-autonomous effect, any inhibition observed by L-canavanine would be attributed to a neural circuit-based mechanism. Despite its lack of impact on spike rate, addition of L-canavanine to a sucrose stimulus inhibited the sweet GRN calcium response (Figure 4A). Moreover, this inhibition was blocked by the addition of the $GABA_BR$ antagonist CGP54626 to the brain (Figure 4B) and significantly blunted by knockdown of *$GABA_BR2$* expression in sweet GRNs (Figure 4C). Together, these data suggest a model in which activation of bitter GRNs by L-canavanine results in increased GABA release in the SEZ and subsequent inhibition of sweet GRN output via $GABA_BR$ (Figure 4G). To test this model behaviorally, we measured the inhibition of PER by increasing concentrations of L-canavanine after *$GABA_BR2$* knockdown in sweet GRNs. Remarkably, knockdown of *$GABA_BR2$* almost completely blocked the inhibition of PER by L-canavanine (Figure 4D). As further confirmation, we also tested PER inhibition by denatonium, a compound that activates bitter GRNs and also acts through OBP49a to directly inhibit sugar receptors [25, 26]. Here we observed only a partial block in PER inhibition, as expected by the dual action of denatonium on bitter and sweet GRN activity (Figure 4E). Notably, knockdown of *$GABA_BR2$* in bitter GRNs by *Gr66a-Gal4* had no effect on PER inhibition (Figure 4F).

We have presented evidence for a gain control mechanism in the fly taste system that differentially affects GRN populations. Sweet neurons receive $GABA_BR$-mediated presynaptic

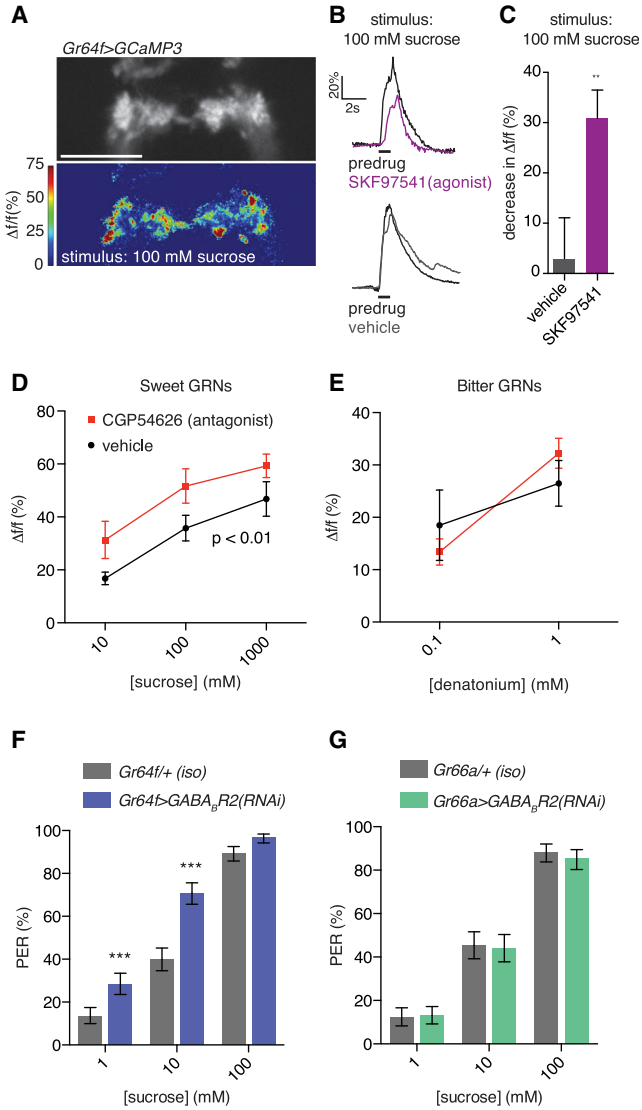

Figure 3. $GABA_BR$ Mediates Presynaptic Inhibition of Sweet GRNs

(A) Baseline fluorescence of sweet GRN axon terminals in the SEZ expressing GCaMP3 under the control of *Gr64f-Gal4* (top) and heatmap showing peak fluorescence changes after stimulation of the proboscis with 100 mM sucrose (bottom). Scale bar, 25 μm.

(B) Representative traces of fluorescence changes in Gr64f axon terminals after stimulation with 100 mM sucrose prior to (black) or after addition of the $GABA_BR$ agonist SKF97541 (magenta) or vehicle alone (gray).

(C) Decrease in peak fluorescence change during stimulation with 100 mM sucrose from addition of SKF97541 (magenta bar) or vehicle alone (gray bar). Graph represents mean ± SEM (n = 17–19 flies) and asterisks indicate significance by t test (**p < 0.01).

(D and E) Average GCaMP3 peak fluorescence changes in Gr64f (D) or Gr66a (E) axon terminals after stimulation with increasing concentrations of sucrose (D) or denatonium (E) in the presence of the $GABA_BR$ antagonist CGP54626 (red) or vehicle alone (black). Graphs represent mean ± SEM (n = 13–15 flies for each concentration). p value indicates significant difference between CGP54626 and vehicle by two-way ANOVA.

(F and G) Sucrose PER responses of flies with *$GABA_BR2$* knocked down in sweet GRNs with *Gr64f-Gal4* (F, blue bars) or bitter GRNs with *Gr66a-Gal4* (G, green bars) compared to each Gal4 line crossed to an isogenic control RNAi line (F and G, gray bars). Graphs represent percentage of stimulations resulting in a positive response ± 95% binomial confidence interval (n = 168–172 flies for F and n = 126–130 flies for G), and asterisks indicate significant change from control (*p < 0.05, **p < 0.01, and ***p < 0.001 by Fisher's exact test with Bonferroni correction for multiple comparisons).

See also Figure S3.

inhibition, which expands their dynamic range, whereas bitter neurons lack $GABA_BR$ expression and therefore retain maximal sensitivity. Importantly, sweet GRN gain control also mediates suppression of sugar responses in the presence of bitter compounds. Intermodal inhibition (termed "mixture suppression") has also been observed in mammalian taste coding, in which responses of parabrachial nucleus and gustatory cortex neurons to mixtures of appetitive and aversive stimuli are most often similar to or smaller than the response to the most effective component of the mixture alone [28–31]. Although inhibitory connections between taste channels have been proposed to underlie these effects, our study provides the first direct evidence for such a mechanism in any animal.

The observed suppression of sweet responses by bitter compounds also raises an interesting question about the behavioral role of bitter detection in flies because bitter aversion is generally assessed in the context of an appetitive stimulus, most often as a reduced attraction to sugar [9, 10, 21, 25, 32–34]. What proportion of this behavioral response to bitter compounds is due to reduced sweet neuron output, either through inhibition of the sweet receptors or presynaptic inhibition of the sweet GRNs, versus dedicated higher-order bitter circuits mediating avoidance? A more complete understanding of taste circuit wiring and function is necessary to fully answer this question. It will also be important to better understand the roles of presynaptic inhibition in other neuron classes. Pheromone-sensitive ORNs in the olfactory system have been observed to receive high levels of presynaptic inhibition, suggesting that this may be a general principle of pheromone detection [5]. Whether gain control of *ppk23*-expressing GRNs mediates suppression of pheromone responses by other sensory inputs could reveal important insights into pheromone processing, courtship, and aggression.

Experimental Procedures

Fly Stocks

Flies were raised on standard cornmeal fly food at 25°C and 70% relative humidity. The following fly lines were used: *$GABA_BR2$-Gal4* and *UAS-$GABA_BR2$(RNAi)#2* [5]; *LexAop-CD2::GFP* [35]; *Gr64f-LexA::VP16* [36]; *Gr66a-LexA::VP16* and *ppk28-LexA::VP16*, *UAS-CD8::tdTomato* [7]; *Gr64f-Gal4* [20]; *Gr66a-Gal4* [10]; *GAD1-Gal4*; *Gr5a-LexA::VP16*, *UAS-CD4::spGFP1-10*, and *LexAop-CD4::spGFP11* [9]; *UAS-GCaMP3* [37]; and *w^{1118}*, *UAS-wntD(RNAi)*, *UAS-Ccap(RNAi)*, and *UAS-$GABA_BR2$(RNAi)* (TRiP collection, Bloomington Stock Center).

Immunohistochemistry

Antibody staining of brains and proboscis labella was carried out as previously described [9, 10]. The following primary antibodies were used: mouse anti-GFP (1:100, Sigma #G6539), rabbit anti-GFP (1:1000, Invitrogen #A11122), rabbit anti-DsRed (1:500 for detecting tdTomato, Clontech #632496), and nc82 (1:50, DSHB). The secondary antibodies used were goat anti-mouse Alexa-488, goat anti-mouse Alexa-568, goat anti-rabbit Alexa-488, and goat anti-rabbit Alexa-488 (Invitrogen). Confocal z stacks were acquired using a Leica SP5 II confocal microscope with a 63× oil-immersion objective.

Behavioral Assays

PER was performed as previously described [9]. Adult female flies aged 3–10 days were starved on water-saturated Kimwipes at 25°C for 22–24 hr before testing. After flies were mounted on strips of myristic acid, they were allowed to recover in a humidified chamber for 1–2 hr. Before testing, each fly was stimulated with water on the tarsi of the foreleg and allowed to drink ad libitum. Testing commenced once none of the flies responded to water after two consecutive foreleg stimulations. For concentration curves, each fly was stimulated on the foreleg for 500 ms with the indicated tastant, which was removed before the proboscis could make contact. Water was

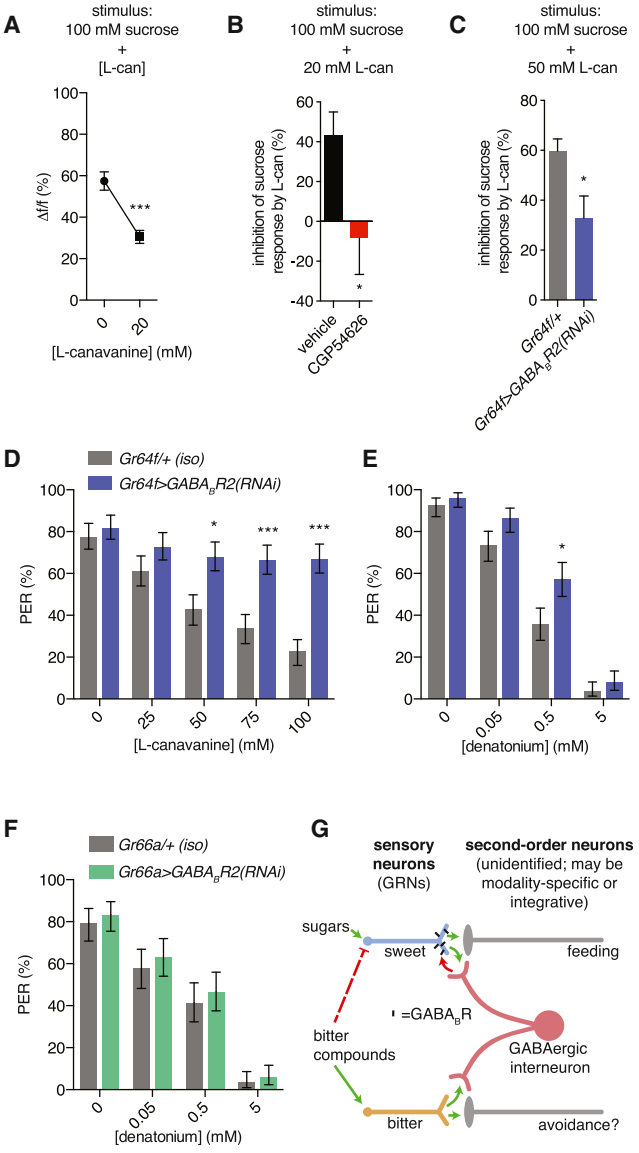

Figure 4. $GABA_BR$ Mediates Suppression of Sugar Responses by Bitter Stimuli

(A) Average peak fluorescence changes in sweet GRN axon terminals (*Gr64f-Gal4*, *UAS-GCaMP3*) after stimulation with 100 mM sucrose plus or minus 20 mM L-canavanine.

(B) Inhibition of sweet GRN calcium response by L-canavanine, in the presence of vehicle (black bar) or $GABA_BR$ antagonist CGP54626 (red bar). Inhibition measured as percent decrease in calcium response evoked by 100 mM sucrose plus 20 mM L-canavanine relative to prior stimulation with 100 mM sucrose alone.

(C) Inhibition of sweet GRN calcium response by L-canavanine in control flies (gray bar) and flies with *$GABA_BR2$* knocked down in *Gr64f*-expressing neurons (blue bar). Inhibition was measured as the percent decrease in calcium response evoked by 100 mM sucrose plus 50 mM L-canavanine relative to prior stimulation with 100 mM sucrose alone. L-canavanine was used at 50 mM for this experiment because of the more robust behavioral effects seen in (D).

(A–C) Graphs represent the mean ± SEM (n = 11 flies). Asterisks indicate significant difference from 0 mM L-canavanine value in (A) and from controls in (B) and (C) by t test (*p < 0.05, **p < 0.01, and ***p < 0.001).

(D–F) PER inhibition by L-canavanine (D) or denatonium (E and F) in flies with *$GABA_BR2$* knocked down in sweet GRNs with *Gr64f-Gal4* (D and E, blue bars) or bitter GRNs with *Gr66a-Gal4* (F, green bars) compared to each Gal4 line crossed to an isogenic control RNAi line (D–F, gray bars). All stimuli contain 100 mM sucrose plus indicated concentration of bitter compound. Graphs represent percentage of stimulations resulting in a positive response ± 95% binomial confidence interval (n = 94 flies for D, n = 76 flies for E, and n = 60 flies for F). Asterisks indicate significant change from control (*p < 0.05, **p < 0.01, and ***p < 0.001 by Fisher's exact test with Bonferroni correction for multiple comparisons).

(G) Model for sweet-bitter integration. Some, but not all, bitter compounds directly inhibit sweet GRNs (dashed red line). $GABA_BR$ expressed by sweet GRNs mediates gain control and suppression of sweet GRNs after bitter GRN activation. Still-unidentified higher-order circuits that control feeding (gray) are illustrated as modality-specific but may include points of further integration. Green arrows indicate activation; red arrows indicate inhibition.

offered between stimulations to wash tarsi and keep flies water satiated. Each tastant was tested twice consecutively, and the number of extensions per fly was recorded. Flies were offered 1 M sucrose at the end of each experiment to confirm viability; flies that did not respond were discarded from the data set. Control animals for RNAi experiments consisted of *Gr64f-Gal4* or *Gr66a-Gal4* crossed to one of two isogenic RNAi lines from the same RNAi collection targeting genes known to lack expression in taste neurons: *UAS-Ccap(RNAi)* or *UAS-wntD(RNAi)*. The two control RNAi lines gave indistinguishable results.

GCaMP Imaging

Female flies aged 2–12 days were briefly anesthetized, and all legs were removed to allow unobstructed access to the proboscis. With a custom chamber, each fly was mounted by insertion of the cervix into individual collars. For further immobilization of the head, nail polish was applied in a thin layer to seal the head to the chamber. Melted wax was applied with a modified dental waxer to adhere the fully extended proboscis to the chamber rim. The antennae and the associated cuticle covering the SEZ were removed, and adult hemolymph-like (AHL) buffer with ribose [38, 39] was immediately injected into the preparation to cover the exposed brain. The esophagus was clipped to allow clear imaging of the SEZ. A coverslip was inserted into the chamber to keep the proboscis dry and separate from the preparation. For pharmacology experiments, a tear was made in the perineural sheath using freshly sharpened forceps. The sheath was pinched near the antennal lobe to prevent damage to the SEZ. After pinching, forceps were quickly tugged away from the brain to produce a small hole, allowing access of drugs to the brain.

GCaMP3 fluorescence was imaged with a Leica SP5 II laser scanning confocal microscope equipped with a tandem scanner and HyD detector. The relevant area of the SEZ was visualized using the 25× water objective with an electronic zoom of 4 (GAD1 imaging) or 8 (taste projection imaging). Images were acquired at a speed of 8,000 lines per second with a line average of 4, resulting in a collection time of 131 ms per frame at a resolution of 512 × 512 pixels or 60 ms per frame at a resolution of 512 × 200 pixels. The pinhole was opened to 2.68–4 Airy units (AU). For each taste stimulation, images were acquired for 10 s prior to stimulation, approximately 1 s during stimulation, and at least 9 s after stimulation.

Prior to recording, a pipette tip filled with 1–2 μl of taste solution was positioned close to the proboscis labellum. After 10 s of recording, the pipette was moved with a manually controlled micromanipulator to make contact with the labellum. Taste solutions were dissolved in distilled water and used at the indicated concentrations. Between taste stimulations, the pipette tip was rinsed with water.

The maximum change in fluorescence (Δf/f) was calculated as follows: (peak average intensity over five frames after stimulation − average intensity over ten frames prior to stimulation) / average intensity over ten frames prior to stimulation. Quantification of fluorescence changes was performed using Microsoft Excel.

Pharmacology

CGP54626 hydrochloride (Tocris) is a silent competitive $GABA_BR$ antagonist used previously in fly heterologous cells [6], in cultured neurons [40], and in vivo [3, 5]. It was dissolved as a 50 mM stock in DMSO and used at a final concentration of 25 μM. SKF97541 (Tocris) is a selective $GABA_BR$ agonist that is roughly ten times more potent than baclofen or 3-APPA [41] and has been used effectively to modulate sensory neuron output in the fly olfactory system [5, 42]. It was kept as a 100 mM stock in 100 mM NaCl and used at a final concentration of 20 μM. The appropriate volume of each drug was first diluted in AHL buffer to make a 4×–5× solution and then added to the preparation to achieve the final concentration. Drugs were added directly into the AHL solution bathing the brain between 1–5 min prior to taste stimulation.

Tastants

The sugars D-sucrose (Fisher BioReagents) and D-glucose (Sigma) were kept as 1 M stocks in water and diluted to the desired concentrations for PER and calcium imaging experiments. The bitter compounds L-canavanine (from *Canavalia ensiformis*, jack bean) and denatonium benzoate were both obtained from Sigma-Aldrich and kept as 1 M stocks dissolved in water. L-canavanine was stored at 4°C.

Statistical Analyses

For PER analyses, the 95% binomial confidence interval was calculated using JavaStat (http://statpages.org/confint.html). Fisher's exact tests were calculated using Graphpad QuickCalcs (http://www.graphpad.com/quickcalcs/). All other statistical tests were performed using GraphPad Prism 6 software.

Supplemental Information

Supplemental Information includes three figures and can be found with this article online at http://dx.doi.org/10.1016/j.cub.2014.07.020.

Author Contributions

B.C. performed and analyzed the majority of experiments. V.C. performed the $GABA_BR$ expression analysis in the labellum. K.M. assisted with the design and implementation of pharmacology experiments. M.D.G designed and supervised the project and wrote the paper with input from B.C., V.C., and K.M.

Acknowledgments

We thank J. Wang and D. Nassel for sharing $GABA_BR$ reagents; K. Scott, H. Amrein, and the Bloomington Stock Center for fly strains; the Developmental Studies Hybridoma Bank for antibodies; M. Hiroi for designing and building the calcium imaging chamber; and P. Cameron for comments on the manuscript. This work was funded by Canadian Institutes of Health Research (CIHR) grant MOP-114934 and the Canadian Foundation for Innovation (CFI). M.D.G. is a CIHR New Investigator.

Received: May 6, 2014
Revised: June 16, 2014
Accepted: July 9, 2014
Published: August 14, 2014

References

1. Yarmolinsky, D.A., Zuker, C.S., and Ryba, N.J.P. (2009). Common sense about taste: from mammals to insects. Cell *139*, 234–244.
2. Scott, K. (2005). Taste recognition: food for thought. Neuron *48*, 455–464.
3. Olsen, S.R., and Wilson, R.I. (2008). Lateral presynaptic inhibition mediates gain control in an olfactory circuit. Nature *452*, 956–960.
4. Olsen, S.R., Bhandawat, V., and Wilson, R.I. (2010). Divisive normalization in olfactory population codes. Neuron *66*, 287–299.
5. Root, C.M., Masuyama, K., Green, D.S., Enell, L.E., Nässel, D.R., Lee, C.-H., and Wang, J.W. (2008). A presynaptic gain control mechanism fine-tunes olfactory behavior. Neuron *59*, 311–321.
6. Mezler, M., Müller, T., and Raming, K. (2001). Cloning and functional expression of GABA(B) receptors from Drosophila. Eur. J. Neurosci. *13*, 477–486.
7. Thistle, R., Cameron, P., Ghorayshi, A., Dennison, L., and Scott, K. (2012). Contact chemoreceptors mediate male-male repulsion and male-female attraction during Drosophila courtship. Cell *149*, 1140–1151.
8. Toda, H., Zhao, X., and Dickson, B.J. (2012). The Drosophila female aphrodisiac pheromone activates ppk23(+) sensory neurons to elicit male courtship behavior. Cell Rep *1*, 599–607.
9. Gordon, M.D., and Scott, K. (2009). Motor control in a Drosophila taste circuit. Neuron *61*, 373–384.
10. Wang, Z., Singhvi, A., Kong, P., and Scott, K. (2004). Taste representations in the Drosophila brain. Cell *117*, 981–991.
11. Ito, K., Shinomiya, K., Ito, M., Armstrong, J.D., Boyan, G., Hartenstein, V., Harzsch, S., Heisenberg, M., Homberg, U., Jenett, A., et al.; Insect Brain Name Working Group (2014). A systematic nomenclature for the insect brain. Neuron *81*, 755–765.
12. Feinberg, E.H., Vanhoven, M.K., Bendesky, A., Wang, G., Fetter, R.D., Shen, K., and Bargmann, C.I. (2008). GFP Reconstitution Across Synaptic Partners (GRASP) defines cell contacts and synapses in living nervous systems. Neuron *57*, 353–363.
13. Inoshita, T., and Tanimura, T. (2006). Cellular identification of water gustatory receptor neurons and their central projection pattern in Drosophila. Proc. Natl. Acad. Sci. USA *103*, 1094–1099.
14. Chen, Z., Wang, Q., and Wang, Z. (2010). The amiloride-sensitive epithelial Na+ channel PPK28 is essential for Drosophila gustatory water reception. J. Neurosci. *30*, 6247–6252.
15. Cameron, P., Hiroi, M., Ngai, J., and Scott, K. (2010). The molecular basis for water taste in Drosophila. Nature *465*, 91–95.
16. Inagaki, H.K., Ben-Tabou de-Leon, S., Wong, A.M., Jagadish, S., Ishimoto, H., Barnea, G., Kitamoto, T., Axel, R., and Anderson, D.J. (2012). Visualizing neuromodulation in vivo: TANGO-mapping of dopamine signaling reveals appetite control of sugar sensing. Cell *148*, 583–595.
17. Wilson, R.I., and Laurent, G. (2005). Role of GABAergic inhibition in shaping odor-evoked spatiotemporal patterns in the Drosophila antennal lobe. J. Neurosci. *25*, 9069–9079.
18. Dethier, V.G. (1976). The Hungry Fly: A Physiological Study of the Behavior Associated with Feeding (Cambridge: Harvard University Press).
19. Hiroi, M., Meunier, N., Marion-Poll, F., and Tanimura, T. (2004). Two antagonistic gustatory receptor neurons responding to sweet-salty and bitter taste in Drosophila. J. Neurobiol. *61*, 333–342.
20. Dahanukar, A., Lei, Y.T., Kwon, J.Y., and Carlson, J.R. (2007). Two Gr genes underlie sugar reception in Drosophila. Neuron *56*, 503–516.
21. Marella, S., Fischler, W., Kong, P., Asgarian, S., Rueckert, E., and Scott, K. (2006). Imaging taste responses in the fly brain reveals a functional map of taste category and behavior. Neuron *49*, 285–295.
22. Slone, J., Daniels, J., and Amrein, H. (2007). Sugar receptors in Drosophila. Curr. Biol. *17*, 1809–1816.
23. Farhadian, S.F., Suárez-Fariñas, M., Cho, C.E., Pellegrino, M., and Vosshall, L.B. (2012). Post-fasting olfactory, transcriptional, and feeding responses in Drosophila. Physiol. Behav. *105*, 544–553.
24. Suh, G.S.B., Wong, A.M., Hergarden, A.C., Wang, J.W., Simon, A.F., Benzer, S., Axel, R., and Anderson, D.J. (2004). A single population of olfactory sensory neurons mediates an innate avoidance behaviour in Drosophila. Nature *431*, 854–859.
25. Meunier, N., Marion-Poll, F.D.R., Rospars, J.-P., and Tanimura, T. (2003). Peripheral coding of bitter taste in Drosophila. J. Neurobiol. *56*, 139–152.
26. Jeong, Y.T., Shim, J., Oh, S.R., Yoon, H.I., Kim, C.H., Moon, S.J., and Montell, C. (2013). An odorant-binding protein required for suppression of sweet taste by bitter chemicals. Neuron *79*, 725–737.
27. Hiroi, M., Tanimura, T., and Marion-Poll, F. (2008). Hedonic taste in Drosophila revealed by olfactory receptors expressed in taste neurons. PLoS ONE *3*, e2610.
28. Vogt, M.B., and Smith, D.V. (1993). Responses of single hamster parabrachial neurons to binary taste mixtures of citric acid with sucrose or NaCl. J. Neurophysiol. *70*, 1350–1364.
29. Vogt, M.B., and Smith, D.V. (1994). Responses of single hamster parabrachial neurons to binary taste mixtures of NaCl with sucrose or QHCl. J. Neurophysiol. *71*, 1373–1380.
30. Maier, J.X., and Katz, D.B. (2013). Neural dynamics in response to binary taste mixtures. J. Neurophysiol. *109*, 2108–2117.
31. Vogt, M.B., and Smith, D.V. (1993). Responses of single hamster parabrachial neurons to binary taste mixtures: mutual suppression between sucrose and QHCl. J. Neurophysiol. *69*, 658–668.
32. Thorne, N., Chromey, C., Bray, S., and Amrein, H. (2004). Taste perception and coding in Drosophila. Curr. Biol. *14*, 1065–1079.
33. Weiss, L.A., Dahanukar, A., Kwon, J.Y., Banerjee, D., and Carlson, J.R. (2011). The molecular and cellular basis of bitter taste in Drosophila. Neuron *69*, 258–272.
34. Sellier, M.-J., Reeb, P., and Marion-Poll, F. (2011). Consumption of bitter alkaloids in Drosophila melanogaster in multiple-choice test conditions. Chem. Senses *36*, 323–334.
35. Lai, S.L., and Lee, T. (2006). Genetic mosaic with dual binary transcriptional systems in Drosophila. Nat. Neurosci. *9*, 703–709.
36. Miyamoto, T., Slone, J., Song, X., and Amrein, H. (2012). A fructose receptor functions as a nutrient sensor in the Drosophila brain. Cell *151*, 1113–1125.

37. Tian, L., Hires, S.A., Mao, T., Huber, D., Chiappe, M.E., Chalasani, S.H., Petreanu, L., Akerboom, J., McKinney, S.A., Schreiter, E.R., et al. (2009). Imaging neural activity in worms, flies and mice with improved GCaMP calcium indicators. Nat. Methods *6*, 875–881.
38. Wang, J.W., Wong, A.M., Flores, J., Vosshall, L.B., and Axel, R. (2003). Two-photon calcium imaging reveals an odor-evoked map of activity in the fly brain. Cell *112*, 271–282.
39. Liu, C., Plaçais, P.-Y., Yamagata, N., Pfeiffer, B.D., Aso, Y., Friedrich, A.B., Siwanowicz, I., Rubin, G.M., Preat, T., and Tanimoto, H. (2012). A subset of dopamine neurons signals reward for odour memory in Drosophila. Nature *488*, 512–516.
40. Hamasaka, Y., Wegener, C., and Nässel, D.R. (2005). GABA modulates Drosophila circadian clock neurons via GABAB receptors and decreases in calcium. J. Neurobiol. *65*, 225–240.
41. Seabrook, G.R., Howson, W., and Lacey, M.G. (1990). Electrophysiological characterization of potent agonists and antagonists at pre- and postsynaptic GABAB receptors on neurones in rat brain slices. Br. J. Pharmacol. *101*, 949–957.
42. Ignell, R., Root, C.M., Birse, R.T., Wang, J.W., Nässel, D.R., and Winther, A.M.E. (2009). Presynaptic peptidergic modulation of olfactory receptor neurons in Drosophila. Proc. Natl. Acad. Sci. USA *106*, 13070–13075.